Distribution of the Gamow-Teller strength in ^{90}Nb and ^{208}Bi

A. Krasznahorkay,[1,2] H. Akimune,[3] M. Fujiwara,[1,4] M. N. Harakeh,[5] J. Jänecke,[6] V. A. Rodin,[5,7] M. H. Urin,[1,7] and M. Yosoi[1]

[1]*Research Center for Nuclear Physics, Osaka University, Mihogaoka 10-1 Ibaraki, Osaka 657-0047, Japan*
[2]*Institute of Nuclear Research of the Hungarian Academy of Science, P.O. Box 51, H-4001 Debrecen, Hungary*
[3]*Department of Physics, Konan University, Higashinada, Kobe 658-8501, Japan*
[4]*Advanced Science Research Center, Japan Atomic Energy Research Institute, Tokai, Ibaraki 319-1195, Japan*
[5]*Kernfysisch Versneller Instituut, 9747 AA Groningen, The Netherlands*
[6]*Department of Physics, University of Michigan, Ann Arbor, Michigan 48109-1120*
[7]*Moscow Engineering Physics Institute, RU-115409 Moscow, Russia*

(Received 24 April 2001; published 12 November 2001)

The (^{3}He,t) charge-exchange reaction has been studied at $E(^3\mathrm{He})=450$ MeV and angles near 0° on targets of ^{90}Zr and ^{208}Pb. Fragmentation of the Gamow-Teller (GT) strength into separate components of the particle-hole type has been observed. The distribution of the GT strength in ^{90}Nb and in ^{208}Bi has been calculated within the continuum quasiparticle random phase approximation and continuum-random-phase approximation approaches, respectively. These components, especially in ^{208}Pb, could be related with the direct, core polarization, and back-spin-flip Gamow-Teller strength.

DOI: 10.1103/PhysRevC.64.067302 PACS number(s): 24.30.Cz, 25.55.Kr, 27.80.+w, 27.60.+j

The Gamow-Teller (spin-flip, isospin-flip) transition has played an important role in nuclear physics. It was first recognized as a component of the weak interaction in allowed β decay. Later, it was found that the initial step of the hydrogen fusion reaction leading to nucleosynthesis, the electron-capture reactions leading to stellar collapse and supernova formation [1] were mediated by this Gamow-Teller (GT) transition. Basic understanding for all these processes requires the reliable knowledge on the GT strength distribution at relatively low excitation energies.

From the systematic retardation of the allowed β decays in nuclei, the presence of the GT resonances at high excitation energies was theoretically predicted [2]. In 1980, the giant GT resonance was actually found to be preferentially excited in the (p,n) reactions at high bombarding energies [3]. Detailed experimental investigations of GT resonances have already been started in the early 1970s [4–6]. A GT resonance consisting of 1^+ states of maximum collectivity should appear at high excitation energies. Those states are mainly associated with charge-exchange excitations of neutrons from orbits with $j_>=l+1/2$ into protons in the spin-orbit partner orbits with $j_<=l-1/2$. Considerations involving the Wigner supermultiplet coupling scheme [7] and the spin-isospin characteristics place these GT excitations at energies near the respective isobaric analog states. If the Wigner SU(4) symmetry is assumed to be exact, the energies of isobaric analog states and the Gamow-Teller resonances would be equal, and these resonances would exhaust entirely the corresponding sum rules. Under this assumption, fragmentation of the Gamow-Teller resonance into states of the particle-hole type would not exist. Within the framework of the shell model, the Wigner SU(4) symmetry is broken mainly by the spin-orbit term of the nuclear mean field.

The possible existence of low-lying less collective Gamow-Teller fragments was predicted on the basis of a quasiclassical treatment within the framework of the random-phase approximation (RPA) [8,9]. Two fragments based on core-polarization spin-flip ($j_<\rightarrow j_<$ or $j_>\rightarrow j_>$) and back-spin-flip ($j_<\rightarrow j_>$) are expected. The latter type of excitation is present only in neutron-rich nuclei when the proton orbits for a lower-lying spin-orbit partner are not completely filled [9].

The GT strength distribution of ^{90}Nb has been investigated by Bainum *et al.* [3] using ^{90}Zr(p,n) reaction at $E_p=120$ MeV, but their energy resolution full width at half maximum [(FWHM)=660 keV] was not sufficient to resolve the transitions to the low-lying excited states in ^{90}Nb.

The GT strength distribution of ^{208}Bi was investigated by Flanders *et al.* [10] using again (p,n) reaction with a somewhat better energy resolution of FWHM=430 keV.

The aim of the present work was to study the fragmentation of the GT strengths into low-lying excited states in ^{90}Nb and in ^{208}Bi using better energy resolution and higher statistics than previously used. Furthermore, theoretical calculations were performed to identify the low-lying parts of the GT strength including the contributions of the core polarization and back-spin-flip. As applied to ^{208}Bi, the calculation results were described in Ref. [11].

The experiment was carried out at the Research Center for Nuclear Physics (RCNP), Osaka University. A 450 MeV $^3\mathrm{He}^{2+}$ beam extracted from the RCNP ring cyclotron was achromatically transported to the ^{90}Zr and ^{208}Pb targets with a thickness of ≈ 5 mg/cm^2 and isotopic enrichments of 98% and 99.9%, respectively. The typical beam intensity was 2–5 e nA. The beam spot size on the target was about 1 mm×1 mm. The emittance of the beam was ~2 mrad (FWHM). The halo of the beam was monitored by measuring the counting rates in plastic scintillators arranged at several points along the beam transport line.

The momentum and energy of the ejectile tritons were measured with the magnetic spectrometer "Grand Raiden" [12]. The spectrometer was set at −0.3° with opening angles, which were defined by a slit at the entrance of the

 ©2001 The American Physical Society

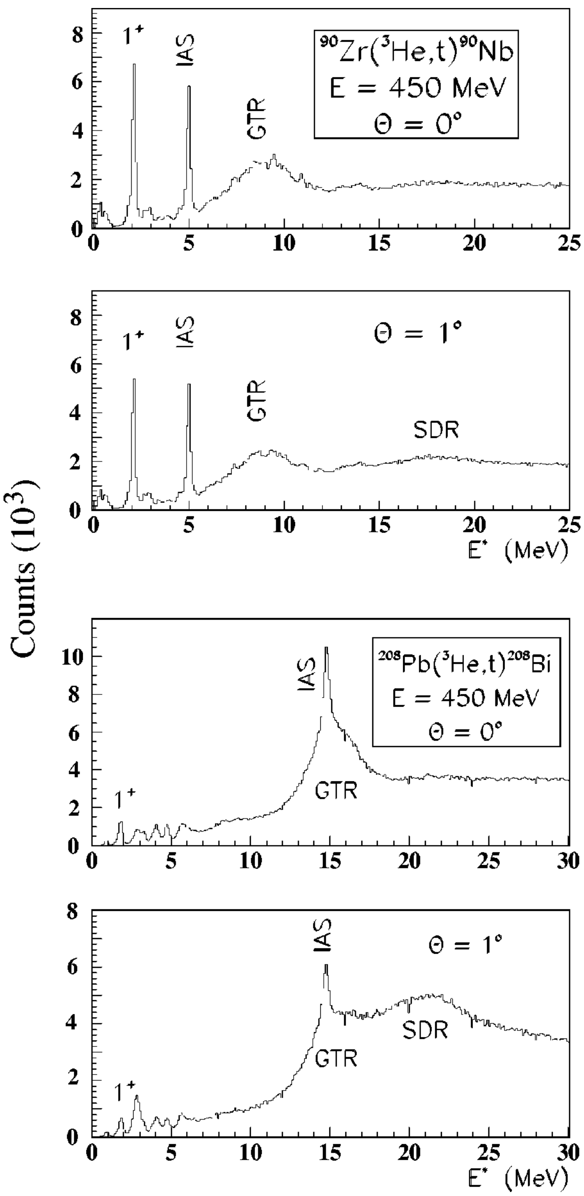

FIG. 1. (^{3}He,t) energy spectra for ^{90}Zr and ^{208}Pb. The positions of the 1^+ states, IAS, the GTR, and the spin-flip dipole resonances (SDR) are indicated.

spectrometer, of ± 20 mrad horizontally, and ± 20 mrad vertically. The spectrometer covered an angular range from $-1.45°$ to 0.85°. The 0° and 1° spectra were generated offline, using equal solid angles of $\Omega = 0.28$ msr, defined by a horizontal opening angle $\Delta\theta_h = \pm 0.40°$, and a vertical opening angle, $\Delta\theta_v = \pm 0.57°$ centered at 0° and 1°. Using this solid angle, the contribution of the dipole strength in the "0° spectra" did not increase to an extent that would harm the separation of monopole and dipole strength. This can be easily assessed from comparing the "0° and 1° spectra" in Fig. 1, where the difference in $L=1$ contributions in both spectra is prominent. Furthermore, as mentioned later, $L=1$ contributions to the "0° spectra" could be removed by subtracting a properly weighted 1° spectrum. The transmission of scattered particles passing through the spectrometer with this solid angle was confirmed to be 100% in other (p,p') and (^{3}He,^{3}He$'$) measurements performed independently. The incident ^{3}He^{2+} beam was stopped by a Faraday cup positioned inside of the $D1$ magnet.

The ejectile tritons were detected with two multiwire drift chambers (MWDC's) [13] placed along the focal plane with a tilting angle of 45° with respect to the central ray of the spectrometer. The MWDC's were 1150 mm long and 45 mm high. One MWDC was placed at the focal plane of the spectrograph and the other MWDC was placed at a distance of 250 mm downstream from the first one. Each MWDC consisted of two planes to measure the horizontal and vertical positions of the incident charged particles. The position and angular resolutions of the MWDC's were 0.3 mm and 1.2 mrad, respectively.

The MWDC's were backed by two ΔE plastic scintillators with a thickness of 5 mm each. These scintillators were used for particle identification. The resulting triton spectra for ^{90}Nb and ^{208}Bi are shown in Fig. 1. The achieved energy resolution was 300 keV.

All spectra measured at 0° show a strong peak corresponding to singly ionized ^{3}He$^+$ ions at 450 MeV produced by atomic charge-exchange reactions in the target [14]. This peak has been used, together with the known Q value of the ground state and the excitation energy of the isobaric analog states (IAS) relative to the ground state, for calibration of the energy scale and the angle of incidence, since the energy and angular distribution of the ^{3}He$^+$ particles are identical to those of the incident ^{3}He^{2+} beam.

The spectra measured at 0° with respect to the beam direction contain almost exclusively the $L=0$ strengths. A small admixture mostly from $L=1$ components is eliminated by subtracting the strengths measured at 1°, where the $L=1$ strengths have their maximum, from the strengths measured at 0°.

The decomposition of the spectra into resonances and nonresonant components, as shown in Fig. 2, makes use of a fitting procedure invoking analytical equations. The resonances are described by assuming Breit-Wigner and also Gaussian shapes for the energy distributions involving three free parameters each: the centroid energies, the widths, and the heights. The uncertainty caused by the different line shapes in the determination of the intensities is taken into account in the error bars. For the quasi-free continuum (QFC) background, the following relationship is used [15]:

$$\frac{d^2\sigma_{\rm QF}}{dE\,d\Omega} = N_{\rm QF}\frac{1-\exp[(E_{\rm t}-E_0)/T]}{1+[(E_{\rm t}-E_{\rm QF})/W]^2}. \qquad (1)$$

Only $N_{\rm QF}$ and $E_{\rm QF}$ are used as free parameters. The other variables were fixed to the recommended values in Ref. [15].

The spectra measured at 0° and 1° were fitted simultaneously using the same shape parameters for the resonances and for the background and only the amplitudes were considered to be independent in the two spectra. The energy and width of the spin-flip dipole resonance obtained from the present analysis are in good agreement with the previous experimental data [16,17]. Although the resonance peaks

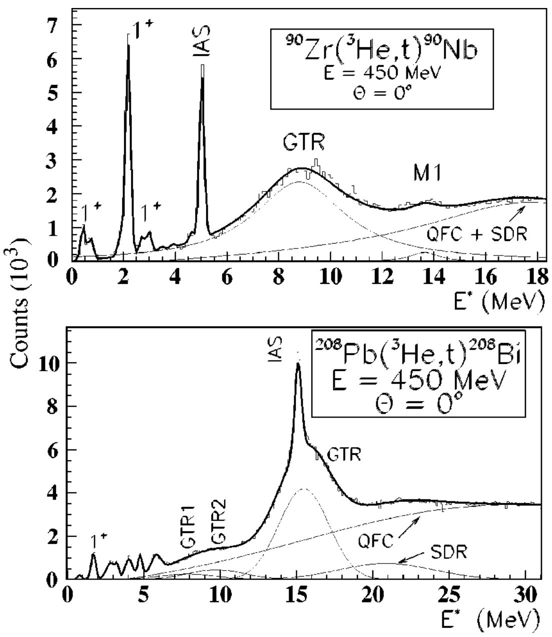

FIG. 2. Zero-degree (^{3}He,t) energy spectra for ^{90}Zr and ^{208}Pb isotopes. The positions of the 1^+ states, IAS, the GTR, and SDR are indicated together with the QFC background. The solid lines through the data are results of fits with Lorentzian line shapes for ^{90}Nb and Gaussian line shapes for ^{208}Bi as described in the text.

around 1°, its contribution was necessary to take into account also at 0° in order to get a good fit.

The level scheme of ^{90}Nb has been compiled recently [18]. The assignment of the proton-neutron multiplet states was mostly based on γ-branching ratios following the (p,n) reaction using a very small (10 cm^3) Ge(Li) detector [19]. Below $E_x = 2.5$ MeV, six $J^\pi = 1^+$ levels were found that are nearly equivalent to the seven states all expected from the possible 1^+ states of a $[\pi(p_{1/2})^a(g_{9/2})^{3-a}\nu(p_{1/2})^b(g_{9/2})^{11-b}]_{0\leqslant a\leqslant 2,1\leqslant b\leqslant 2}$ configuration [19]. From the β decay of ^{90}Mo, there are four levels for which the log ft values are smaller than 5.1 [20]. A $J^\pi = 1^+$ level in ^{90}Nb with a large ^{90}Zr(^{3}He,t)^{90}Nb cross section should coincide with a level with a small log ft value when there is no configuration

TABLE I. Relative GT strengths of the low-lying levels in ^{90}Nb and ^{208}Bi compared to the strengths of the main Gamov-Teller resoance (GITR) (*) complex peak.

^{90}Nb		^{208}Bi	
E_x (MeV)	I_{GT}/I_{GTR} (%)	E_x (MeV)	I_{GT}/I_{GTR} (%)
0.36(5)	2.9(5)		
1.82(5)	1.9(6)	1.80(3)	2.7(5)
2.13(5)	18.8(15)	3.2(1)	0.7(4)
2.67(5)	1.4(6)	4.1(1)	3.0(5)
2.95(5)	1.8(6)	4.7(1)	1.8(5)
3.4(2)	0.2(2)	5.9(2)	3.2(8)
3.9(2)	0.3(3)	8.0(2)	7 (3)
4.6(1)	0.9(5)	9.8(2)	12(4)
8.8(2)	100.0(GTR)	15.6(2)	100.0(GTR)

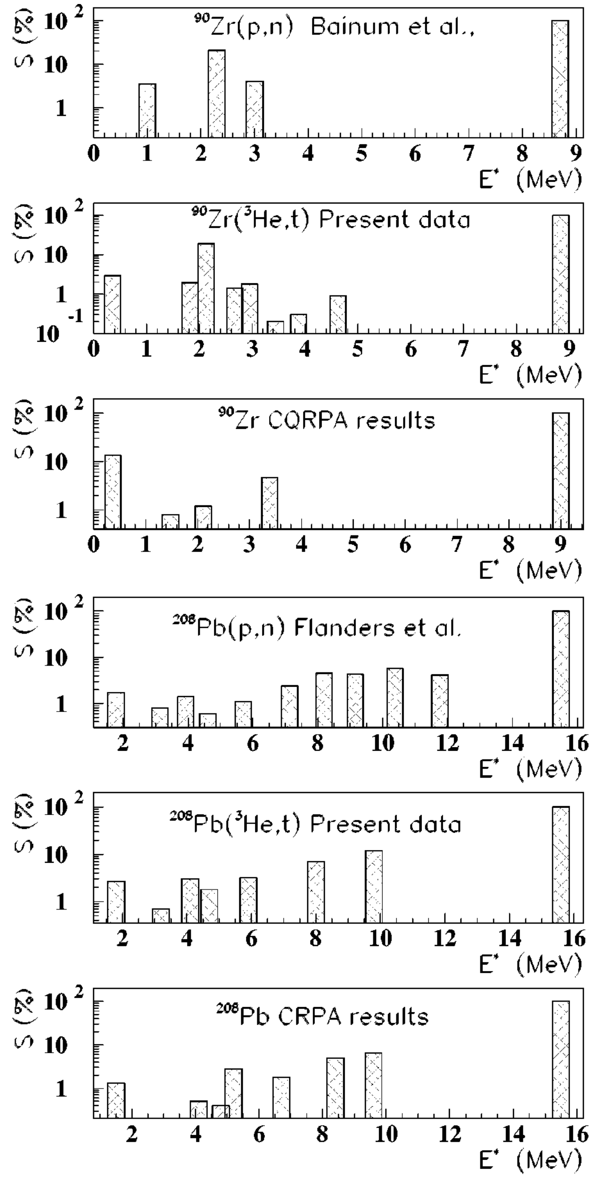

FIG. 3. Relative GT strength $[S = I_{GT}/I_{GTR}$ (%)] deduced from (^{3}He,t) energy spectra for ^{90}Zr and ^{208}Pb isotopes, compared with the results calculated in continuum quasiparticle random phase approximation (CQRPA) and in continuum-random-phase approximation (CRPA), respectively.

(seniority) mixing for a 1^+ state. Taking into account the (^{3}He,t) results obtained at low bombarding energy [21], this is clearly not the case. There is considerable configuration mixing as is also indicated by the ^{90}Mo β^+ decay and electron-capture data. Only one level at the excitation energy of 2125.6 keV has a large (^{3}He,t) cross section and a small log ft value. Hence, this state is considered to be dominantly $(\pi 1g_{9/2})(\nu 1g_{9/2})^{-1}$ configuration. The GT strengths determined in this work are summarized in Table I. The uncertainties of the energies and strengths are also indicated in parentheses.

The GT strengths determined in this work may be compared to the previous results of Bainum *et al.* [3] in Fig. 3. Taking into account their worse energy resolution and a small miscalibration of the spectra at low excitation energy, the agreement of the data is acceptable. However, with the factor 2 better energy resolution and seven times higher statistics achieved in the present experiment and we were able to map the strength distribution in a more detailed way.

^{208}Bi is one of the best nuclei to study the proton-neutron residual interaction. The low-lying states in ^{208}Bi have been studied using many different transfer and compound reactions and many proton-neutron multiplet states have been assigned [22]. However, only a few 1^+ states could be tentatively identified. The first (1^+) state has been found at 1802.5 keV and was identified as the 1^+ member of the $(\pi 2f_{7/2})(\nu 2f_{5/2})^{-1}$ multiplet [22]. This state has been excited very strongly in the (^{3}He,t) reaction at $\theta=0°$ (see Fig. 1 and Fig. 2) confirming the above identification. Above this state we observed six smaller peaks that may belong mainly to the $(\pi 3p_{3/2})(\nu 3p_{1/2})^{-1}$, $(\pi 3p_{1/2})(\nu 3p_{3/2})^{-1}$, $(\pi 1i_{11/2})\times(\nu 1i_{13/2})^{-1}$, and $(\pi 2f_{5/2})(\nu 2f_{7/2})^{-1}$, etc., proton-neutron multiplets according to the proton-particle [23] and neutron-hole states [24] observed in ^{209}Bi and in ^{207}Pb, respectively. Their relative strengths are summarized in Table I.

The GT strengths of ^{208}Bi determined in the present work can be compared with the strengths determined by Flanders *et al.* [10] and Jänecke *et al.* [25]. As shown in Fig. 3, the agreement of the data with the ones measured by Flanders *et al.* below 6 MeV is acceptable, but there is a disagreement at higher energies. They assumed five different peaks between 6 and 12 MeV, but with our better resolution and statistics we could get a good fit by assuming only two broader ones. However, the total intensity in the whole 6–12 MeV energy region agrees well. The agreement of the relative strengths with the data of Jänecke *et al.* [25] is good below 5.6 MeV. Above 5.6 MeV they did not publish any GT strengths.

The distribution of the GT strength has been calculated within a continuum version of the quasiparticle-RPA approach taking into account the proton pairing and the (p,n) particle-particle interactions. The approach will be described elsewhere. A larger number of the low-energy weakly collective GT states [as compared with just one low-energy GT state within continuum-random-phase approximation (CRPA)] appears in the continuum quasiparticle random phase approximation (CQRPA) calculations as a result of the proton paring in ^{90}Zr. The distribution of the GT strengths in ^{208}Bi has been calculated within the continuum-RPA approach described in Ref. [11]. The choice of model parameters (parameters of the phenomenological mean field, dimensionless strengths of the isovector part of the Landau-Migdal particle-hole interaction) and partial self-consistency conditions are also described in Ref. [11]. The GT strength functions have been calculated up to $E^*=9$ and 16 MeV for ^{90}Nb and ^{208}Bi, respectively, and are compared to the experimental ones in Fig. 3.

The most interesting result concerning the distribution of the GT strengths in ^{208}Bi might be the identification of two rather collective states at $E^*=8.0$ and 9.8 MeV. These states are related to the two GT states, named core polarization and back spin flip, found by a schematic analysis of the corresponding RPA equations rather long ago [9]. The total GT strength of the above states calculated in the present work is in satisfactory agreement with our experimental data.

The energy and strength of weakly collective GT states with energies $E^*\leqslant 7$ MeV are described rather poorly due to the schematic shell model (nuclear mean field and particle-hole interaction) used in the present work. However, the total relative strength of these states can be reasonably compared with the corresponding experimental value. Such a comparison seems satisfactory.

This work was supported in part by the Ministry of Education, Science, Sports, and Culture of Japan (Monbusho), by the U.S. National Science Foundation (NSF), by the Japan Society for Promotion of Science (JSPS) under the U.S.-Japan Cooperative Science Program, the Hungarian OTKA Foundation No. N32570, and the Nederlandse Organisatie voor Wetenschapelijk Onderzoek.

[1] W.P. Alford and B.M. Spicer, Adv. Nucl. Phys. **24**, 1 (1998).
[2] J.I. Fujita and K. Ikeda, Nucl. Phys. **67**, 145 (1965).
[3] D.E. Bainum *et al.*, Phys. Rev. Lett. **44**, 1751 (1980).
[4] C. Gaarde and T. Kammuri, Nucl. Phys. **A215**, 314 (1973).
[5] W.R. Wharton and P.D. Debevec, Phys. Lett. **51B**, 447 (1974); Phys. Rev. C **11**, 1963 (1975).
[6] A. Galonsky *et al.*, Phys. Rev. C **14**, 748 (1976).
[7] E.P. Wigner, Phys. Rev. **51**, 106 (1937); **56**, 519 (1939).
[8] Yu.V. Gaponov and Yu.S. Lyutostanskii, Phys. At. Nucl. **19**, 62 (1974).
[9] Yu.V. Gaponov and Yu.S. Lyutostanskii, Phys. Part. Nucl. **12**, 1234 (1981).
[10] B.S. Flanders *et al.*, Phys. Rev. C **40**, 1985 (1989).
[11] E.A. Moukhai, V.A. Rodin, and M.H. Urin, Phys. Lett. B **447**, 8 (1999).
[12] M. Fujiwara *et al.*, Nucl. Instrum. Methods Phys. Res. A **422**, 484 (1999).
[13] T. Noro *et al.*, RCNP Annual Report 1991.
[14] K. Dennis *et al.*, Phys. Rev. A **50**, 3992 (1994).
[15] J. Jänecke *et al.*, Phys. Rev. C **48**, 2828 (1993).
[16] C. Gaarde *et al.*, Nucl. Phys. **A369**, 258 (1981).
[17] H. Akimune *et al.*, Phys. Rev. C **61**, 011304(R) (2000).
[18] E. Browne, Nucl. Data Sheets **82**, 379 (1987).
[19] Y. Yoshida *et al.*, Nucl. Phys. **A187**, 161 (1972).
[20] J.A. Cooper *et al.*, Nucl. Phys. **A109**, 603 (1967).
[21] S.I. Hayakawa *et al.*, Nucl. Phys. **A139**, 465 (1969).
[22] M.J. Martin, Nucl. Data Sheets **47**, 797 (1986).
[23] M.J. Martin, Nucl. Data Sheets **63**, 768 (1991).
[24] M.R. Schmorak, Nucl. Data Sheets **43**, 418 (1994).
[25] J. Jänecke *et al.*, Nucl. Phys. **A526**, 1 (1991).